

# ON THE PRANDTL-KOLMOGOROV 1-EQUATION MODEL OF TURBULENCE

KIERA KEAN<sup>1</sup>, WILLIAM LAYTON<sup>2</sup>, AND MICHAEL SCHNEIER<sup>3</sup>

**ABSTRACT.** We prove an estimate of total (viscous plus modelled turbulent) energy dissipation in general eddy viscosity models for shear flows. For general eddy viscosity models, we show that the ratio of the near wall average viscosity to the effective global viscosity is the key parameter. This result is then applied to the 1-equation, URANS model of turbulence for which this ratio depends on the specification of the turbulence length scale. The model, which was derived by Prandtl in 1945, is a component of a 2-equation model derived by Kolmogorov in 1942 and is the core of many unsteady, Reynolds averaged models for prediction of turbulent flows. Away from walls, interpreting an early suggestion of Prandtl, we set

$$l = \sqrt{2}k^{+1/2}\tau,$$

where  $\tau$  = selected time scale. In the near wall region analysis suggests replacing the traditional  $l = 0.41d$  ( $d$  = wall normal distance) with  $l = 0.41d\sqrt{d/L}$  giving, e.g.,

$$l = \min \left\{ \sqrt{2}k^{+1/2}\tau, 0.41d\sqrt{\frac{d}{L}} \right\}.$$

This  $l(\cdot)$  results in a simpler model with correct near wall asymptotics. Its energy dissipation rate scales no larger than the physically correct  $O(U^3/L)$ , balancing energy input with energy dissipation.

## 1. INTRODUCTION

Predicting turbulent flows in practical settings means solving models intended to predict averages of solutions of the Navier-Stokes (NS) equations. Among a wide variety of approaches, summarized in Wilcox [38], eddy viscosity URANS (unsteady Reynolds Averaged NS) models are used in many applications. Many are based on the 1-equation model of Prandtl [26] and Kolmogorov [17], considered herein and given by

$$(1) \quad \begin{aligned} v_t + v \cdot \nabla v - \nabla \cdot ([2\nu + \nu_T(\cdot)] \nabla^s v) + \nabla p &= f(x, y, z), \\ \nabla \cdot v &= 0, \text{ and } \nu_T = \mu l \sqrt{k}, \\ k_t + v \cdot \nabla k - \nabla \cdot ([\nu + \nu_T(\cdot)] \nabla k) + \frac{1}{l} k \sqrt{k} &= \nu_T(\cdot) |\nabla^s v|^2. \end{aligned}$$

Following for example [22] and [38] p.37 eq. (3.9),  $v$  approximates a finite time window average of the Navier-Stokes velocity  $u$

$$(2) \quad v(x, y, z, t) \simeq \bar{u}(x, y, z, t) = \frac{1}{\tau} \int_{t-\tau}^t u(x, y, z, t') dt'.$$

The fluctuation is  $u' = u - \bar{u}$ . Its associated turbulent kinetic energy, approximated by the  $k$ -equation solution, is  $k_{true} = \frac{1}{2} |u - \bar{u}|^2(x, y, z, t)$ . In (1)  $\nu$  is the kinematic

viscosity,  $p$  is a pressure, initial and boundary conditions for  $v$  and  $k$  will be specified,  $f$  is the body force (here  $f = 0$ ),  $\nabla^s v$  is the symmetric part of  $\nabla v$  and  $\nu_T(\cdot)$  is the eddy viscosity. The  $k$ -equation is derived, for example, in [3] p.99, Section 4.4, [5], [22] p.60, Section 5.3 or [25] p.369, Section 10.3. The term  $\nabla \cdot (\nu \nabla k)$  in the  $k$ -equation is included in the model by some and considered negligible by others.

The Kolmogorov-Prandtl relation is  $\nu_T = \mu l \sqrt{k}$  where  $\mu$  is a calibration constant, typically 0.2 to 0.6, and often 0.55, [5] p. 114,[25]. The turbulence length-scale  $l = l(x, y, z, t)$  is specified to complete the model. In current practice,  $l(\cdot)$  varies from model to model, subregion to subregion (requiring their locations, [29]) and must be specified by the user; see [38], [15] for many examples.

This lack of a simple, effective, and universal specification of  $l(\cdot)$  is one disadvantage of 1-equation models like (1). Another disadvantage, shared by many eddy viscosity models, is that model dissipation often exceeds energy input and leads to lower Reynolds number solutions. Herein we analyze a specification of  $l$  with greater universality and improved model dissipation

$$(3) \quad l = \min \left\{ \sqrt{2}k^{+1/2}\tau, 0.41d\sqrt{\frac{d}{L}} \right\}, \text{ where}$$

$d =$  wall distance,  $\tau =$  averaging window,  $L =$  global length scale.

The main result herein, Theorem 4.1 Section 4, is that with (3) for shear flows, this over dissipation does not happen: the model's energy dissipation rate is consistent with its energy input rate. The effect of the minimum in (3) is to select  $l = \sqrt{2}k^{+1/2}\tau$  in the flow's interior and the new value  $l = 0.41d\sqrt{d/L}$  near walls. (Other realizations of this intent are possible, e.g., (5).) The traditional value of the Von Karman constant, 0.41, is retained in (3). Prandtl [27] described  $l(\cdot)$  as "*... the diameter of the masses of fluid moving as a whole in each individual case*". This diameter is constrained by nearby walls leading to the classical  $l = 0.41d$  and here  $0.41d\sqrt{d/L}$ . Prandtl also mentioned a second possibility, "*...or again, as the distance traversed by a mass of this type before it becomes blended in with neighboring masses...*" This remark can be interpreted as  $l = |u'(x, t)|\tau$ , i.e., the distance a fluctuating eddy travels in one time unit. As  $|u'| \simeq \sqrt{2}k^{+1/2}$ , away from walls we specify the kinematic relation

$$(4) \quad l(\cdot) = \sqrt{2}k(\cdot)^{+1/2}\tau.$$

**1.1. Justification of  $l = 0.41d\sqrt{d/L}$ .** The (dimensionally consistent) near wall  $l = 0.41d\sqrt{d/L}$  is a deviation from accepted practice, so justification is necessary. The true turbulent kinetic energy  $k_{true} = \frac{1}{2}\overline{|u - \bar{u}|^2} \rightarrow 0$  like  $O(d^2)$  at walls. This rate implies that  $k_{true}$  satisfies

$$k_{true} = 0 \text{ and } \nabla k_{true} \cdot n = 0 \text{ at the wall.}$$

The eddy viscosity should have a similar near wall behavior since, modulo pressure terms,  $\mu l \sqrt{k} \nabla^s v \simeq u'u' \rightarrow 0$  at walls like  $O(d^2)$ . If  $k_{true}$  replaces  $k$  in  $\nu_T(\cdot)$ , then  $\mu l \sqrt{k_{true}} \nabla^s v = O(d^2)$  near walls with  $l = 0.41d$ . However, the solution to the  $k$ -equation satisfies only one boundary condition,  $k = 0$  at the wall. Thus, the solution to the  $k$  equation (intended to model  $k_{true}$ ) has only

$$k = 0 \text{ at the wall, and } k(d) = O(d) \text{ as the wall is approached.}$$

This (incorrectly) implies  $\mu l \sqrt{k} \nabla^s v \rightarrow 0$  at walls like  $O(d^{+1.5})$  when  $l = 0.41d$ . This is one reason for evaluations such as Pope [25] p. 434 Section 11.7.2 that " ... the specification  $l = 0.41y$  is too large in the near wall region..." as well as ad hoc addition of van Driest damping. The modification  $l = 0.41d\sqrt{d/L}$  in (3) ensures  $\nu_T(\cdot) = O(d^2)$  correctly in the model.

The question arises of why not simply specify  $l(\cdot) = \sqrt{2}k(\cdot)^{+1/2}\tau$  as in [20]. The positive results in [20] were for turbulence induced by a body force with  $f(x) = 0$  on  $\partial\Omega$  which excludes shear flows. The physical difference in the settings (summarizing the introduction of Phillips [24]) is that in shear flows the near wall region produces small scales which dominate  $k_{true}$ , while when shear flows are excluded in [20], small scales are produced only through the nonlinearity.

**1.2. Related work.** The energy dissipation rate is a fundamental statistic of turbulence, e.g., [25], [35]. Its balance with energy input rates,  $\langle \varepsilon \rangle = \mathcal{O}(U^3/L)$ , is observed in physical experiments [35]. In 1992, Doering and Constantin [8] established a direct link between phenomenology and NSE predicted energy dissipation through upper bounds consistent with the  $\mathcal{O}(U^3/L)$  rate. This work builds on [2], [13] and has developed in many important directions, e.g., [7], [13], [35], [36], [16], [37]. Remarkably, an  $\mathcal{O}(U^3/L)$  lower bound has recently been proven in [4] for stochastically forced shear flow.

Model over-dissipation, producing a lower  $\mathcal{R}e$  flow, is due to the action of turbulent viscosity terms on small scales generated by breakdown of large scales through the nonlinearity or in the boundary layer.  $\langle \varepsilon \rangle$  has been analyzed for some simpler models, e.g., [18], [19] (showing a dramatic difference between shear and no shear cases), and [23]. The kinematic length scale  $l = \sqrt{2}k^{+1/2}\tau$  occurred naturally in an ensemble algorithm in [14] and was highly developed by Teixeira and Cheinet [32] and [33] (see equation (7) on p. 2699), with near-wall transition to  $l = 0.41d$  by

$$(5) \quad l = \theta(0.41d) + (1 - \theta) \left( \sqrt{2}k^{+1/2}\tau \right), \text{ with } \theta = e^{-d/100}.$$

The global specification  $l = \sqrt{2}k^{+1/2}\tau$  was proven in [20] not to over-dissipate with shear excluded (and boundary layers negligible). This work leads to the problem considered herein to analyze shear/boundary layer induced model dissipation.

Since  $\tau$  in (2), (3) is user supplied, it can be determined by the time scales required in an application or related to a time step. The latter blurs the line between URANS and time filtered large eddy simulation, [28], as noted in the abstract of [9] "...most of the unsteady approaches ... can be regarded as a temporally filtered approach." The time scale  $\tau$  can also be regarded as a fundamental time scale of turbulence such as  $\tau = k/\varepsilon$ , e.g., [30]. Other natural choices of  $\tau$  include  $\tau \simeq \delta/U$ ,  $\delta =$  an estimate of layer-width [32] and  $\tau = 0.76/N$ ,  $N =$  a selected-frequency, [6].

## 2. SHEAR FLOW

We analyze energy dissipation caused by the boundary layer for shear flow with zero body force, building on analysis in the pioneering paper [8] and early work of Hopf [12]. Let the flow domain  $\Omega = (0, L)^3$  and select  $L$ -periodic boundary conditions in  $x, y$  and no-slip at  $z = 0, z = L$ . The wall is fixed at  $z = 0$  and the

wall at  $z = L$  slides with velocity  $(U, 0, 0)$ :

$$(6) \quad \begin{array}{ll} \textit{Boundary} & \textit{Conditions} : \\ \text{moving top lid:} & v(x, y, L, t) = (U, 0, 0) \\ \text{fixed bottom wall:} & v(x, y, 0, t) = 0 \\ \text{periodic side walls:} & v(x + L, y, z, t) = v(x, y, z, t), \\ & v(x, y + L, z, t) = v(x, y, z, t). \end{array}$$

On this domain the wall normal distance is  $d = \min\{z, L - z\}$ . Since time averages of the velocity satisfy the same shear boundary conditions as the NSE solution, the correct boundary condition for  $k(x, y, z, t)$  is

$$k(x, y, 0, t) = k(x, y, L, t) = 0 \text{ and } L - \text{periodicity in } x, y.$$

Since  $k$  has homogeneous boundary conditions, non-zero initial conditions must be specified; otherwise, if  $k(x, y, z, 0) = 0$ , then  $k(x, y, z, t) \equiv 0$  thereafter.

**2.1. Notation and preliminaries.** The  $L^2(\Omega)$  norm and the inner product are  $\|\cdot\|$  and  $(\cdot, \cdot)$ . The  $L^p(\Omega)$  norms are  $\|\cdot\|_{L^p}$ .  $C$  represents a generic positive constant independent of  $\nu, Re$ , and other model parameters.

**Definition 2.1.** *The finite and long time averages of a function  $\phi(t)$  are*

$$\langle \phi \rangle_T = \frac{1}{T} \int_0^T \phi(t) dt \text{ and } \langle \phi \rangle_\infty = \limsup_{T \rightarrow \infty} \langle \phi \rangle_T.$$

These satisfy  $\langle \langle \phi \rangle_\infty \rangle_\infty = \langle \phi \rangle_\infty$  and

$$(7) \quad \langle \phi \psi \rangle_T \leq \langle |\phi|^2 \rangle_T^{1/2} \langle |\psi|^2 \rangle_T^{1/2}, \quad \langle \phi \psi \rangle_\infty \leq \langle |\phi|^2 \rangle_\infty^{1/2} \langle |\psi|^2 \rangle_\infty^{1/2}.$$

A weak solution of the model momentum equation for shear flow problem satisfies the initial condition and

$$(8) \quad (v_t, w) + ([2\nu + \nu_T(\cdot)] \nabla^s v, \nabla^s w) + (v \cdot \nabla v, w) = 0$$

for all test functions  $w$ , with  $\nabla \cdot w = 0$ ,  $L$ -periodic in  $x$  and  $y$  and  $w(x, y, 0, t) = 0, w(x, y, L, t) = 0$ . If  $\phi$  is a divergence free function extending the shear boundary conditions (6) into  $\Omega$ , formally taking the inner product with  $w = v - \phi$  and expanding gives

$$\begin{aligned} & \frac{1}{2} \frac{d}{dt} \|v\|^2 + \int_\Omega [2\nu + \nu_T(\cdot)] |\nabla^s v|^2 dx = \\ & = (v_t, \phi) + \int_\Omega [2\nu + \nu_T(\cdot)] \nabla^s v : \nabla^s \phi dx + (v \cdot \nabla v, \phi). \end{aligned}$$

**Definition 2.2.** *The total energy dissipation rate (per unit volume) is*

$$\varepsilon(v) = \frac{1}{|\Omega|} \int_\Omega [2\nu + \nu_T(\cdot)] |\nabla^s v(x, t)|^2 dx.$$

While a new  $l(\cdot)$  gives a new model, existence of weak solutions to models of this type is treated comprehensively in [3] and [1]. Herein, we assume that a weak solution of the model (1), (3) with shear boundary conditions (6) exists,  $k \geq 0$  and solutions satisfy the energy inequality

$$(9) \quad \begin{aligned} & \frac{1}{2} \frac{d}{dt} \|v\|^2 + \int_\Omega [2\nu + \nu_T(\cdot)] |\nabla^s v|^2 dx \leq \\ & (v_t, \phi) + \int_\Omega [2\nu + \nu_T(\cdot)] \nabla^s v : \nabla^s \phi dx + (v \cdot \nabla v, \phi). \end{aligned}$$

Using the energy inequality the appendix gives a proof of the following bounds.

**Proposition 2.1** (Uniform Bounds). *Consider the 1-equation model (1), (3) with shear boundary conditions (6). The following are uniformly bounded in  $T$ :*

$$\|v(T)\|^2, \int_{\Omega} k(T)dx, \int_{\Omega} \nu_T(\cdot, T)dx, \\ \left\langle \frac{1}{L^3} \int_{\Omega} |\nabla^s v|^2 dx \right\rangle_T, \left\langle \frac{1}{L^3} \int_{\Omega} \frac{1}{l} k \sqrt{k} dx \right\rangle_T, \left\langle \frac{1}{L^3} \int_{\Omega} [2\nu + \nu_T(\cdot)] |\nabla^s v|^2 dx \right\rangle_T.$$

### 3. ENERGY DISSIPATION IN SHEAR FLOWS

To formulate our first main result we first present a definition of the **effective viscosity**  $\nu_{eff}$  ( $\geq \nu$ ), the **average viscosity** in the boundary layer  $\mathcal{S}_{\beta}$ , and a few related quantities. These are well defined due to the uniform bounds in Proposition 2.3.

**Definition 3.1.** *The effective viscosity of solutions of (1) under (6) is*

$$\nu_{eff} := \frac{\left\langle \frac{1}{|\Omega|} \int_{\Omega} [2\nu + \nu_{turb}(\cdot)] |\nabla^s v|^2 dx \right\rangle_{\infty}}{\left\langle \frac{1}{|\Omega|} \int_{\Omega} |\nabla^s v|^2 dx \right\rangle_{\infty}}.$$

The large scale turnover time is  $T^* = L/U$ . The Reynolds number and effective Reynolds number are

$$\mathcal{Re} = \frac{UL}{\nu} \quad \text{and} \quad \mathcal{Re}_{eff} = \frac{UL}{\nu_{eff}}.$$

Let  $\beta = \frac{1}{8}\mathcal{Re}_{eff}^{-1}$  and denote the region  $\mathcal{S}_{\beta}$  by

$$\mathcal{S}_{\beta} = \{(x, y, z) : 0 \leq x \leq L, 0 \leq y \leq L, (1 - \beta)L < z < L\}.$$

The average viscosity,  $\bar{\nu}$ , in  $\mathcal{S}_{\beta}$  is denoted

$$\bar{\nu} := \left\langle \frac{1}{|\mathcal{S}_{\beta}|} \int_{\mathcal{S}_{\beta}} [2\nu + \nu_T(\cdot)] dx \right\rangle_{\infty}, \quad \text{where } |\mathcal{S}_{\beta}| = \beta L^3.$$

Generally, the ratio of the effective and average viscosity is an important statistic.

**Theorem 3.1.** *Suppose  $\nu_T(\cdot) \geq 0$ . Let  $v$  be a weak solution of*

$$v_t + v \cdot \nabla v - \nabla \cdot ([2\nu + \nu_T(\cdot)] \nabla^s v) + \nabla p = 0, \quad \text{and } \nabla \cdot v = 0$$

*under (6) satisfying the energy inequality (9). Then, provided  $\bar{\nu}, \nu_{eff}$  are well defined,*

$$\langle \varepsilon \rangle_{\infty} \leq \left\{ \frac{5}{2} + 8 \frac{\bar{\nu}}{\nu_{eff}} \right\} \frac{U^3}{L}.$$

**Remark 3.1.** *The multiplicative constants 5/2, 8 have not been optimized. Due to the problem symmetries and Galilean invariance, only the upper layer (near  $z = L$ ) needs to be monitored. For general shear flows, the average viscosity  $\bar{\nu}$  should be defined (and thus monitored) as the average over all (here upper and lower) boundary layers present.*

The proof begins with the background flow from Doering and Constantin [8],  $\phi(z) = [\tilde{\phi}(z), 0, 0]^T$  where

$$\tilde{\phi}(z) = \begin{cases} 0, & z \in [0, L - \beta L] \\ \frac{U}{\beta L}(z - (L - \beta L)), & z \in [L - \beta L, L] \end{cases} \quad \beta = \frac{1}{8}\mathcal{R}e_{eff}^{-1}.$$

This function  $\phi(z)$  is piecewise linear, continuous, divergence free and satisfies the boundary conditions. We will need the following values of norms of  $\phi$ .

**Lemma 3.1.** *We have  $\nabla \cdot \phi = 0$  and*

$$\begin{aligned} \|\phi\|_{L^\infty(\Omega)} &= U, & \|\nabla\phi\|_{L^\infty(\Omega)} &= \frac{U}{\beta L}, \\ \|\phi\|^2 &= \frac{1}{3}U^2\beta L^3, & \|\nabla\phi\|^2 &= \frac{U^2L}{\beta}. \end{aligned}$$

With this choice of  $\phi$ , time averaging the energy inequality (9) over  $[0, T]$  and normalizing by  $|\Omega| = L^3$  gives

$$\begin{aligned} (10) \quad & \frac{1}{2TL^3}\|v(T)\|^2 + \left\langle \frac{1}{L^3} \int_{\Omega} [2\nu + \nu_T(\cdot)] |\nabla^s v|^2 dx \right\rangle_T \leq \\ & \leq \frac{1}{2TL^3}\|v(0)\|^2 + \frac{1}{TL^3}(v(T) - v(0), \phi) + \left\langle \frac{1}{L^3}(v \cdot \nabla v, \phi) \right\rangle_T + \\ & \quad + \left\langle \frac{1}{L^3} \int_{\Omega} [2\nu + \nu_T(\cdot)] \nabla^s v : \nabla^s \phi dx \right\rangle_T. \end{aligned}$$

Recall  $\beta = \frac{1}{8}\mathcal{R}e_{eff}^{-1}$ . Due to Proposition 2.3, (10) can be written as

$$(11) \quad \langle \varepsilon \rangle_T \leq \mathcal{O}\left(\frac{1}{T}\right) + \left\langle \frac{1}{L^3}(v \cdot \nabla v, \phi) \right\rangle_T + \left\langle \frac{1}{L^3} \int_{\Omega} [2\nu + \nu_T(\cdot)] \nabla^s v : \nabla^s \phi dx \right\rangle_T$$

The right-hand side (RHS) has two terms shared by the NSE,  $(v \cdot \nabla v, \phi)$  and  $\int 2\nu \nabla^s v : \nabla^s \phi dx$ . The main issue is thus the third term,  $\int \nu_T(\cdot) \nabla^s v : \nabla^s \phi dx$ . Before treating that we recall the analysis of Doering and Constantine [8] and Wang [36] for the first two. For the nonlinear term  $\left\langle \frac{1}{L^3}(v \cdot \nabla v, \phi) \right\rangle_T$ , denoted  $NLT$ , we have

$$\begin{aligned} NLT &= \left\langle \frac{1}{L^3}(v \cdot \nabla v, \phi) \right\rangle_T = \left\langle \frac{1}{L^3}([v - \phi] \cdot \nabla v, \phi) \right\rangle_T + \left\langle \frac{1}{L^3}(\phi \cdot \nabla v, \phi) \right\rangle_T \\ &\leq \left\langle \frac{1}{L^3} \int_{\mathcal{S}_\beta} |v - \phi| |\nabla v| |\phi| + |\phi|^2 |\nabla v| dx \right\rangle_T \\ &\leq \frac{1}{L^3} \left\langle \left\| \frac{v - \phi}{L - z} \right\|_{L^2(\mathcal{S}_\beta)} \|\nabla v\|_{L^2(\mathcal{S}_\beta)} \|(L - z)\phi\|_{L^\infty(\mathcal{S}_\beta)} + \|\phi\|_{L^\infty(\mathcal{S}_\beta)}^2 \|\nabla v\|_{L^1(\mathcal{S}_\beta)} \right\rangle_T. \end{aligned}$$

On the RHS,  $\|\phi\|_{L^\infty(\mathcal{S}_\beta)}^2 = U^2$ . We calculate  $\|(L - z)\phi\|_{L^\infty(\mathcal{S}_\beta)} = \frac{1}{4}\beta LU$ . Since  $v - \phi$  vanishes on  $\partial\mathcal{S}_\beta$ , Hardy's inequality, the triangle inequality and a calculation imply

$$\begin{aligned} \left\| \frac{v - \phi}{L - z} \right\|_{L^2(\mathcal{S}_\beta)} &\leq 2 \|\nabla(v - \phi)\|_{L^2(\mathcal{S}_\beta)} \leq 2 \|\nabla v\|_{L^2(\mathcal{S}_\beta)} + 2 \|\nabla\phi\|_{L^2(\mathcal{S}_\beta)} \\ &\leq 2 \|\nabla v\|_{L^2(\mathcal{S}_\beta)} + 2U \sqrt{\frac{L}{\beta}}. \end{aligned}$$

Thus we have the estimate

(12)

$$NLT \leq \frac{\beta LU}{4} \frac{1}{L^3} \left\langle 2 \|\nabla v\|_{L^2(\mathcal{S}_\beta)}^2 + 2U \sqrt{\frac{L}{\beta}} \|v\|_{L^2(\mathcal{S}_\beta)} \right\rangle_T + \frac{U^2}{L^3} \langle \|\nabla v\|_{L^1(\mathcal{S}_\beta)} \rangle_T.$$

For the last term on the RHS, Hölders inequality in space then in time implies

$$\begin{aligned} \frac{U^2}{L^3} \langle \|\nabla v\|_{L^1(\mathcal{S}_\beta)} \rangle_T &= \frac{U^2}{L^3} \left\langle \int_{\mathcal{S}_\beta} |\nabla v| \cdot 1 dx \right\rangle_T \leq \frac{U^2}{L^3} \left\langle \sqrt{\int_{\mathcal{S}_\beta} |\nabla v|^2 dx} \sqrt{\beta L^3} \right\rangle_T \\ &\leq \frac{U^2 \sqrt{\beta}}{L^{3/2}} \left\langle \sqrt{\int_{\mathcal{S}_\beta} |\nabla v|^2 dx} \right\rangle_T \leq \frac{U^2 \sqrt{\beta}}{L^{3/2}} \left\langle \int_{\mathcal{S}_\beta} |\nabla v|^2 dx \right\rangle_T^{1/2}. \end{aligned}$$

Increase the integral's domain from  $\mathcal{S}_\beta$  to  $\Omega$ , use (as  $\nabla \cdot v = 0$ )  $\|\nabla v\|^2 = 2\|\nabla^s v\|^2$  and  $\beta = \frac{1}{8} \mathcal{R}e_{eff}^{-1}$ . Rearranging and using the arithmetic-geometric inequality gives

$$\begin{aligned} \frac{U^2}{L^3} \langle \|\nabla v\|_{L^1(\mathcal{S}_\beta)} \rangle_T &\leq U^2 \sqrt{\beta} \left\langle \frac{1}{L^3} \int_{\Omega} 2|\nabla^s v|^2 dx \right\rangle_T^{1/2} \leq \\ &\leq U^2 \sqrt{\frac{2}{8} \frac{1}{LU}} \left\langle \frac{1}{L^3} \int_{\Omega} \nu_{eff} |\nabla^s v|^2 dx \right\rangle_T^{1/2} \leq \left(\frac{U^3}{L}\right)^{1/2} \frac{1}{2} \left\langle \frac{1}{L^3} \int_{\Omega} \nu_{eff} |\nabla^s v|^2 dx \right\rangle_T^{1/2} \\ &\leq \frac{1}{2} \frac{U^3}{L} + \frac{1}{8} \left\langle \frac{1}{L^3} \int_{\Omega} \nu_{eff} |\nabla^s v|^2 dx \right\rangle_T. \end{aligned}$$

Similar manipulations yield

$$\begin{aligned} \frac{1}{4} \beta LU \frac{1}{L^3} \left\langle 2U \sqrt{\frac{L}{\beta}} \|v\|_{L^2(\mathcal{S}_\beta)} \right\rangle_T &\leq \frac{1}{2} \beta LU \left\langle \frac{1}{L^3} \|\nabla v\|_{L^2(\mathcal{S}_\beta)}^2 \right\rangle_T + \frac{1}{8} \frac{U^3}{L} \\ &\leq \frac{1}{8} \left\langle \frac{1}{L^3} \nu_{eff} \|\nabla^s v\|_{L^2(\mathcal{S}_\beta)}^2 \right\rangle_T + \frac{1}{8} \frac{U^3}{L}. \end{aligned}$$

Using the last two estimates in the  $NLT$  upper bound (12), we obtain

$$NLT \leq 2\beta \frac{LU}{\nu_{eff}} \left\langle \frac{1}{L^3} \nu_{eff} \|\nabla^s v\|_{L^2(\mathcal{S}_\beta)}^2 \right\rangle_T + \frac{5}{8} \frac{U^3}{L}.$$

Thus,

$$\begin{aligned} \langle \varepsilon \rangle_T &\leq \mathcal{O}\left(\frac{1}{T}\right) + \frac{1}{4} \left\langle \frac{1}{L^3} \nu_{eff} \|\nabla^s v\|_{L^2(\Omega)}^2 \right\rangle_T + \frac{5}{8} \frac{U^3}{L} + \\ &\quad + \left\langle \frac{1}{L^3} \int_{\Omega} [2\nu + \nu_T(\cdot)] \nabla^s v : \nabla^s \phi dx \right\rangle_T. \end{aligned}$$

Consider now the last term on the RHS. Since  $\phi$  is zero off  $\mathcal{S}_\beta$ ,

$$\begin{aligned} \left\langle \frac{1}{L^3} \int_{\Omega} [2\nu + \nu_T(\cdot)] \nabla^s v : \nabla^s \phi dx \right\rangle_T &= \left\langle \frac{1}{L^3} \int_{\mathcal{S}_\beta} [2\nu + \nu_T(\cdot)] \nabla^s v : \nabla^s \phi dx \right\rangle_T \\ &\leq \frac{1}{2} \langle \varepsilon \rangle_T + \frac{1}{2} \left\langle \frac{1}{L^3} \int_{\mathcal{S}_\beta} [2\nu + \nu_T(\cdot)] \left( \frac{U}{\beta L} \right)^2 dx \right\rangle_T \\ &\leq \frac{1}{2} \langle \varepsilon \rangle_T + \frac{1}{2} \left( \frac{U}{\beta L} \right)^2 \beta \left\langle \frac{1}{\beta L^3} \int_{\mathcal{S}_\beta} [2\nu + \nu_T(\cdot)] dx \right\rangle_T. \end{aligned}$$

Thus

$$\begin{aligned} \frac{1}{2} \langle \varepsilon \rangle_T &\leq \mathcal{O}\left(\frac{1}{T}\right) + \frac{1}{4} \left\langle \frac{1}{L^3} \nu_{eff} \|\nabla^s v\|_{L^2(\Omega)}^2 \right\rangle_T + \\ &\quad + \frac{5}{8} \frac{U^3}{L} + \frac{\beta}{2} \left( \frac{U}{\beta L} \right)^2 \left\langle \frac{1}{\beta L^3} \int_{\mathcal{S}_\beta} 2\nu + \nu_T(\cdot) dx \right\rangle_T. \end{aligned}$$

As  $T \rightarrow \infty$

$$\left\langle \frac{1}{\beta L^3} \int_{\mathcal{S}_\beta} 2\nu + \nu_T(\cdot) dx \right\rangle_T \rightarrow \bar{\nu} \text{ and } \left\langle \frac{1}{L^3} \nu_{eff} \|\nabla^s v\|_{L^2(\Omega)}^2 \right\rangle_T \rightarrow \langle \varepsilon \rangle_\infty.$$

Thus,

$$\left( \frac{1}{2} - 2\beta \mathcal{R}e_{eff} \right) \langle \varepsilon \rangle_\infty \leq \frac{5}{8} \frac{U^3}{L} + \frac{1}{2} \left( \frac{U}{\beta L} \right)^2 \beta \bar{\nu} \leq \left[ \frac{5}{8} + \frac{1}{2\beta} \mathcal{R}e_{eff}^{-1} \frac{\bar{\nu}}{\nu_{eff}} \right] \frac{U^3}{L}.$$

The choice  $\beta = \frac{1}{8} \mathcal{R}e_{eff}^{-1}$  implies  $2\beta \mathcal{R}e_{eff} = 1/4$ , completing the proof since

$$\langle \varepsilon \rangle_\infty \leq \frac{5}{2} \frac{U^3}{L} + \frac{1}{2} \left( \frac{U}{\beta L} \right)^2 \beta \bar{\nu} = \left[ \frac{5}{2} + 8 \frac{\bar{\nu}}{\nu_{eff}} \right] \frac{U^3}{L}.$$

#### 4. APPLICATION TO A 1-EQUATION URANS MODEL

We now apply Theorem 3.2 to (1), (3). The main work will be in estimating  $\frac{\bar{\nu}}{\nu_{eff}}$ .

**Theorem 4.1.** *Let  $v$  be a weak solution of (1), (3) under (6) satisfying the energy inequality (9). We have*

$$\langle \varepsilon \rangle_\infty \leq \left[ 5 + 32 \frac{\nu}{\nu_{eff}} + \left( \frac{0.41^2 \sqrt[2]{2} \mu^2}{4} \right) \frac{\tau}{T^*} \right] \frac{U^3}{L}.$$

**Remark.** We note that  $\frac{\nu}{\nu_{eff}} \leq 1$  (and possibly  $\ll 1$ ) and for  $\mu = 0.55$ ,  $0.41^2 \sqrt[2]{2} \mu^2 / 4 \simeq 0.017978$ .



**proof.** The upper bound  $l \leq 0.41d\sqrt{d/L}$  is used in the boundary layer region to estimate  $\bar{\nu}$  as follows

$$\begin{aligned}
 \bar{\nu} &= \left\langle \frac{1}{\beta L^3} \int_{\mathcal{S}_\beta} 2\nu + \nu_T(\cdot) dx \right\rangle_\infty \leq 2\nu + \left\langle \frac{1}{\beta L^3} \int_{\mathcal{S}_\beta} \mu \left( 0.41d\sqrt{\frac{d}{L}} \right) k^{\frac{1}{2}} dx \right\rangle_\infty \\
 &\leq 2\nu + 0.41\mu \frac{1}{L^{+1/2}} \frac{1}{\beta L^3} \left\langle \int_{\mathcal{S}_\beta} (L-z)^{+3/2} k^{+1/2} dx \right\rangle_\infty \\
 &\leq 2\nu + 0.41\mu \frac{1}{L^{+1/2}} \frac{1}{\beta L^3} \left\langle \sqrt{\int_{\mathcal{S}_\beta} (L-z)^3 dx} \sqrt{\int_{\mathcal{S}_\beta} k dx} \right\rangle_\infty \\
 &\leq 2\nu + \frac{0.41\mu}{2} \frac{1}{L^{+1/2}} \beta \left\langle \sqrt{\int_{\mathcal{S}_\beta} k dx} \right\rangle_\infty, \text{ hence} \\
 (13) \quad \bar{\nu} &\leq 2\nu + \frac{0.41\mu}{2} L\beta \sqrt{\left\langle \frac{1}{L^3} \int_{\Omega} k dx \right\rangle_\infty}.
 \end{aligned}$$

Next use the  $k$ -equation to estimate  $\int k dx$ . We have

$$(14) \quad \int_{\Omega} k_t dx + \int_{\Omega} \frac{1}{l} k \sqrt{k} dx = \int_{\Omega} \nu_T(\cdot) |\nabla^s v| dx.$$

By the choice of  $l$ ,  $\frac{1}{l} k \sqrt{k}$  is bounded below by  $\frac{1}{\sqrt{2}\tau} k$  because

$$\frac{1}{l} k \sqrt{k} = \max \left\{ \frac{1}{\sqrt{2}\tau}, \frac{\sqrt{k}}{0.41d\sqrt{\frac{d}{L}}} \right\} k \geq \frac{1}{\sqrt{2}\tau} k.$$

The long time averaging of  $\int k_t dx$  is zero. Since  $\frac{1}{\sqrt{2}\tau} k \leq \frac{1}{l} k \sqrt{k}$ , we have

$$\frac{1}{\sqrt{2}\tau} \left\langle \frac{1}{|\Omega|} \int_{\Omega} k dx \right\rangle_\infty \leq \left\langle \frac{1}{|\Omega|} \int_{\Omega} \frac{1}{l} k \sqrt{k} dx \right\rangle_\infty = \left\langle \frac{1}{|\Omega|} \int_{\Omega} \nu_T(\cdot) |\nabla^s v|^2 dx \right\rangle_\infty = \langle \varepsilon \rangle_\infty.$$

Thus,  $\left\langle \frac{1}{|\Omega|} \int_{\Omega} k dx \right\rangle_\infty \leq \sqrt{2}\tau \langle \varepsilon \rangle_\infty$ . Using this upper estimate in (13) we obtain

$$\bar{\nu} \leq 2\nu + \frac{0.41\mu}{2} L\beta \sqrt{\left\langle \frac{1}{L^3} \int_{\Omega} k dx \right\rangle_\infty} \leq 2\nu + \frac{0.41\sqrt[4]{2}\mu}{2} L\beta\tau^{1/2} \sqrt{\langle \varepsilon \rangle_\infty}.$$

Divide by  $\nu_{eff}$ , use  $T^* = L/U$ ,  $\beta = \frac{1}{8}\mathcal{R}e_{eff}^{-1}$  and rearrange. This gives

$$\frac{\bar{\nu}}{\nu_{eff}} \leq 2 \frac{\nu}{\nu_{eff}} + \frac{0.41\sqrt[4]{2}\mu}{2} \frac{1}{8} \frac{L^{1/2}}{U^{3/2}} \sqrt{\frac{\tau}{T^*}} \sqrt{\langle \varepsilon \rangle_\infty}.$$

Using this estimate in Theorem 3.2 gives

$$\langle \varepsilon \rangle_\infty \leq \left[ \frac{5}{2} + 16 \frac{\nu}{\nu_{eff}} \right] \frac{U^3}{L} + \left[ \frac{0.41\sqrt[4]{2}\mu}{2} \sqrt{\frac{\tau}{T^*}} \sqrt{\frac{U^3}{L}} \right] \sqrt{\langle \varepsilon \rangle_\infty}.$$

The arithmetic-geometric mean inequality then completes the proof:

$$\langle \varepsilon \rangle_\infty \leq \left[ 5 + 32 \frac{\nu}{\nu_{eff}} + \frac{0.41^2 \sqrt[3]{2} \mu^2}{4} \frac{\tau}{T^*} \right] \frac{U^3}{L}.$$

## 5. A NUMERICAL ILLUSTRATION

This section provides a computational illustration of the theoretical results for the model. The results of the computations are consistent with the theoretical predictions. The results were obtained on a workstation with a program developed with the FEniCS software suite [21]. The code can be found on GitHub at <https://github.com/kierakean/1eqnRANS-FEM>.

**5.1. Problem Setting.** We examined the classical Taylor-Couette flow between counter-rotating cylinders for rotations well above, e.g. [10], those yielding stable patterns, [31]. The domain is given by

$$\Omega = \{(x, y, z) : r_{inner}^2 \leq x^2 + y^2 \leq r_{outer}^2, 0 \leq z \leq z_{max}\},$$

with  $r_{inner} = .5, r_{outer} = 1, z_{max} = 2.2$ . Figure 1. (a) depicts the domain  $\Omega$ .

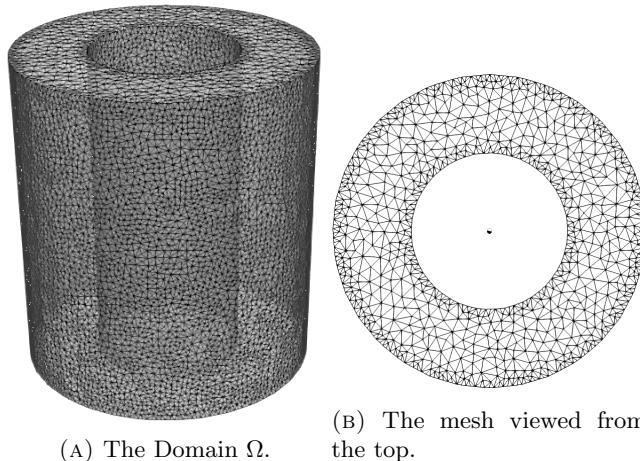


FIGURE 1. The unstructured mesh used in the numerical experiments.

We imposed periodic boundary conditions in the  $z$  direction. The outer cylinder was held fixed and the flow was driven by the rotation of the inner cylinder. The angular velocity of the inner cylinder,  $\omega_{inner}$  was smoothly increased from zero at  $T = 0$  to  $\omega_{inner} = 4$  at  $T = 5$ . Plots of flow statistics indicated that statistical equilibrium was reached around  $T = 20$  so we give snapshots below at  $T = 30$ . We chose final time  $T = 40$  and time averaged over  $20 \leq t \leq 40$ . The time scale was chosen to be  $\tau = 0.1$ .

**Initialization.** The model is turned on with a non-zero  $k(x,5)$  at  $T = 5$  when the inner cylinder has been spun up to its full angular velocity. We use a  $k$  initialization standard for turbulent flow in a square duct, Wilcox [38], given by

$$k(x, 5) = 1.5|v(x, 5)|^2 I^2, \text{ where } I = \text{turbulence intensity} \simeq 0.16\mathcal{R}e^{-1/8}.$$

**The mesh.** We used an unstructured mesh that was refined around the inner and outer boundaries, as can be seen from the top of the mesh in Figure 1 (b). We did preliminary tests at Reynolds number  $\mathcal{R}e = 1000$  by refining the mesh until  $\langle \varepsilon \rangle$

was unchanged on three successive refinements. These parameters yielded a Taylor number of

$$Ta := \frac{\omega^2 r_{inner} (r_{outer} - r_{inner})^3}{\nu^2} = 10^6.$$

We then did all reported tests on the coarsest mesh that produced the same value of  $\langle \varepsilon \rangle$ .

Tests were run with varying Reynolds numbers by varying the viscosity  $\nu$  from  $3 \times 10^{-3}$  to  $5 \times 10^{-4}$  ( $Ta \simeq 10^{10}$  to  $2.5 \times 10^{17}$ ). Persistent vortices, marked by the Q-criterion, are plotted for two Reynolds numbers in Figure 2.

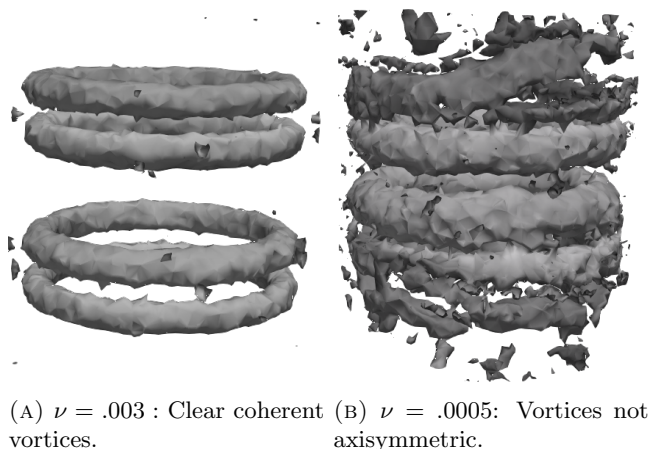


FIGURE 2. Q-criterion at  $T = 30$ .

We used the  $P^2 - P^1$  Taylor-Hood element pair. The velocity space,  $X_h$  and pressure space,  $Q_h$  had 947,802 and 44,585 degrees of freedom, respectively. We used The timestepping scheme backward Euler plus time filter from [11] for the momentum and continuity equation. The added time filter increased accuracy and reduced numerical dissipation making the calculated  $\langle \varepsilon \rangle$  more accurate. We used Backward Euler for the  $k$  equation. This choice smoothed the  $k(x, t)$  evolution and reduced solver issues. We took  $\Delta t = 1e - 2$  and ran the simulation from  $T = 0$  to  $T = 40$ .

**5.2. Energy Dissipation Rate.** In Figure 3  $\varepsilon(t)$  is plotted as a function of time. The jump at  $T = 5$  corresponds to when the  $k$  equation (and thus the turbulent viscosity) is turned on.

To find the dependence on the Reynolds number, we plotted  $\frac{\langle \varepsilon \rangle}{U^3/L}$  as a function of Reynolds number, and fit to  $y = a + bRe^c$  using Matlab's nonlinear least squares tool. The initial guess chosen for the (iterative) solver was  $y = .05 + 5Re^{-1}$ .

Figure 4 shows that the long time average of the energy dissipation rate for the model scales like a constant plus the inverse of the Reynolds number,  $\langle \varepsilon \rangle \simeq (0.5 + 4Re^{-1}) \frac{U^3}{L}$ , consistent with our analysis.

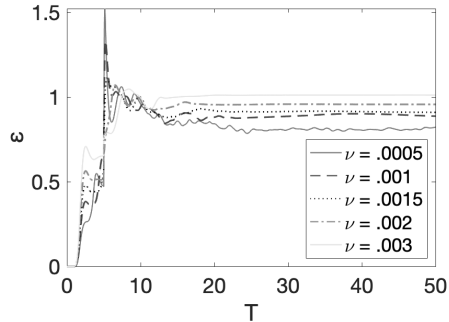


FIGURE 3. The energy dissipation rate over time.

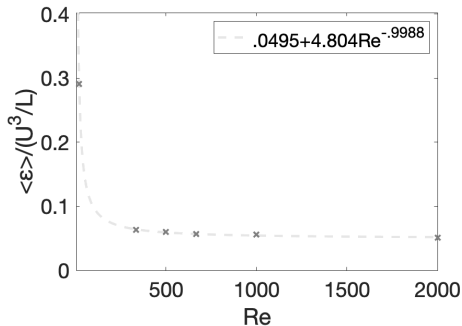


FIGURE 4. The energy dissipation rate over time.

## 6. CONCLUSIONS AND OPEN PROBLEMS

The work herein was motivated by the idea that models more closely reflecting the kinetic energy balance in turbulence can be simpler and require fewer calibration parameters for accuracy. One important aspect of kinetic energy balance is the averaged energy dissipation rate,  $\langle \varepsilon \rangle$ , in turbulence models matching averaged energy input rates,  $U^3/L$ , as they do for the NSE. For (1.1) this matching, related to models not over dissipating solutions, depends on the choice of the turbulence length scale  $l(\cdot)$ , the decision to include or exclude the term  $-\nu \Delta k$  in the  $k$ -equation and (in numerics) numerical dissipation in the methods used. For the turbulence length scale, away from walls we used the simple and universal kinematic specification  $l = \sqrt{2}k^{+1/2}\tau$ . Near walls it is necessary to match the near wall behavior of  $\nu_T(\cdot)$  to that of the Reynolds stress  $-u'u'$ . Including the term  $-\nu \Delta k$ , matching requires near wall behavior  $l = \mathcal{O}(d^{3/2})$ . With this matching, model energy dissipation rates do match input rates, as desired for accuracy. For implementation,  $l = \min \left\{ \sqrt{2}k^{+1/2}\tau, 0.41d\sqrt{d/L} \right\}$  retains the issue of specifying the wall distance but it does not require pre-determining fluid sub-regions.

The 1-equation model studied has been used in many numerical codes, yet open problems abound. The important analytic problems of existence and positivity of  $k$ , while open for the new length scale, seem within reach given the advances in theory presented in Chacon-Rebollo and Lewandowski [3]. The question of inclusion or

exclusion of  $-\nu\Delta k$  is little explored. We conjecture that it is linked to the correct near wall asymptotics of  $l(\cdot)$ , global dissipation rates, and possible ill-posedness of the continuum model and its numerical discretization. The model parameters used in our tests were  $\mu = 0.55$  and von Karman constant 0.41. These values are classical for  $l = 0.41d$ . The numerical illustration found that with these parameter values  $\langle \varepsilon \rangle \simeq (0.5 + 4\mathcal{R}e^{-1}) \frac{U^3}{L}$ . The  $\mathcal{R}e \rightarrow \infty$  limiting value 0.5 includes numerical dissipation and grid effects. It is larger than the best estimate for the NSE of 0.088 of Doering and Constantine [8]. If this persists in more detailed tests, the chosen model parameters 0.55 and 0.41 should be adjusted for the new turbulence length scale herein.

When achievable, the analysis of energy dissipation rates provides a powerful tool to investigate conditions under which turbulence models do not severely over-dissipate solutions. Naturally, the region between models amenable to such analysis and models used in practice remains filled with important, interesting, and challenging open problems.

#### FUNDING

The work of the first and second author was partially supported by NSF grant DMS 1817542.

#### ACKNOWLEDGMENT

We dedicate this paper to Charlie Doering. He was a gifted scientist and to the second author an inspiring colleague.

#### REFERENCES

- [1] M. BULICEK AND J. MALEK, *Large data analysis for Kolmogorov's 2 equation model of turbulence*, *Nonlinear Analysis*. 50 (2018) 104-143.
- [2] F.H. BUSSE, *The optimum theory of turbulence*, *Adv. Appl. Mech.*, 18 (1978), 77-121.
- [3] T. CHACON-REBOLLO AND R. LEWANDOWSKI, *Mathematical and numerical foundations of turbulence models and applications*, Springer, New-York, 2014.
- [4] Y.T. CHOW AND A. PAKZAD, 2020. *On the zeroth law of turbulence for the stochastically forced Navier-Stokes equations*, arXiv preprint, arXiv:2004.08655.
- [5] P. DAVIDSON, *Turbulence: an introduction for scientists and engineers*. Oxford Univ. Press, 2015.
- [6] J.W. DEARDORFF, *Clear and Cloud-Capped Mixed Layers. Their Numerical Simulation, Structure and Growth and Parameterization*, in *Proceedings ECMWF Seminar on the Treatment of the Boundary Layer in Numerical Weather Prediction*, ECMWF, Reading, U.K., pp. 234-284, 1976.
- [7] C.R. DOERING AND C. FOIAS, *Energy dissipation in body-forced turbulence*, *J. Fluid Mech.*, 467 (2002), 289-306.
- [8] C.R. DOERING AND P. CONSTANTIN, *Energy dissipation in shear driven turbulence*, *Phys. Rev. Lett.*, 69.11 (1992): 1648.
- [9] A. FADAI-GHOTBI, C. FRIESS, R. MANCEAU, T.B. GATSKI AND J. BORÉE, *Temporal filtering: A consistent formalism for seamless hybrid RANS-LES modeling in inhomogeneous turbulence*. *International Journal of Heat and Fluid Flow*. 2010 Jun 1;31(3):378-89.
- [10] S. GROSSMANN, D. LOHSE, C. SUN, *High-Reynolds Number Taylor-Couette Turbulence*, *Annual Review of Fluid Mechanics* 2016 48:1, 53-80
- [11] A. GUZEL AND W. LAYTON, *Time filters increase accuracy of the fully implicit method*, *BIT Numerical Mathematics* 58 (2018), 301-315.
- [12] E. HOPF, *On nonlinear partial differential equations*, *Lecture Series Symposium on Partial Differential Equations*, Department of Mathematics, University of Kansas, 1957.

- [13] L.N. HOWARD, *Bounds on flow quantities*, Ann. Rev. Fluid Mech., 4(1972) 473-494.
- [14] NAN JIANG AND W. LAYTON, *Numerical Analysis of two Ensemble Eddy Viscosity Models of Fluid Motion*, Numer. Methods Partial Differ. Equ. 31 (2014) 10.1002/num.21908
- [15] S. KUNDU, M. KUMBHAKAR AND K. GHOSHAL, *Reinvestigation on mixing length in an open channel turbulent flow*, Acta Geophysica, vol. V, 2017 <https://doi.org/10.1007/s11600-017-0109-7>.
- [16] R.R. KERSWELL, *Variational bounds on shear-driven turbulence and turbulent Boussinesq convection*, Physica D 100 (1997), 355–376.
- [17] A.N. KOLMOGOROV, *Equations of turbulent motion in an incompressible fluid*, Izv. Akad. Nauk SSSR, Seria fizicheskaya, 6(1-2):56-58, 1942.
- [18] W. LAYTON, *Bounds on energy dissipation rates of large eddies in turbulent shear flows*, Math. and Comp. Model., 35(2002), 1445-1451.
- [19] W. LAYTON, *Energy dissipation in the Smagorinsky model of turbulence*. Appl. Math. Lett., 59 (2016), 56-9.
- [20] W. LAYTON AND M. MCLAUGHLIN, *On URANS Congruity with Time Averaging: Analytical laws suggest improved models*, in: Proc. International conference in honor of the 90th Birthday of Constantin Corduneanu, Ekaterinburg, Russia (pp. 85-108). Springer, 2018.
- [21] A. LOGG, K. MARDAL, AND G. WELLS, *Automated solution of differential equations by the finite element method: The FEniCS book*, volume 84. Springer Science & Business Media, 2012
- [22] B. MOHAMMADI AND O. PIRONNEAU, *Analysis of the k-epsilon Turbulence Model*, Masson, Paris, 1994.
- [23] A. PAKZAD, *Damping Functions correct over-dissipation of the Smagorinsky Model*, Math. Methods Appl. Sci., 40 (2017), no. 16, DOI 10.1002/mma.4444.
- [24] O.M. PHILLIPS, *Shear Flow Turbulence*, Annual Review of Fluid Mechanics, Volume 1, (1969) 245-264
- [25] S. POPE, *Turbulent Flows*, Cambridge Univ. Press, Cambridge, 2000.
- [26] L. PRANDTL, *Über ein neues Formelsystem für die ausgebildete Turbulenz*, Nacr. Akad. Wiss. Göttingen, Math-Phys. Kl., (1945) 6-16.
- [27] L. PRANDTL, *On fully developed turbulence*, in: Proceedings of the 2nd International Congress of Applied Mechanics, Zurich (1926) 62-74.
- [28] C. PRUETT, *Temporal large-eddy simulation: theory and implementation*. Theoretical and Computational Fluid Dynamics. 2008 May;22(3):275-304.
- [29] P.R. SPALART, *Philosophies and fallacies in turbulence modeling*, Prog. Aerosp. Sci., 74 (2015), 1-15.
- [30] C.G. SPEZIALE, R. ABID AND E.C. ANDERSON, *A critical evaluation of two-equation models for near wall turbulence*, AIAA J. 30(1992) p. 324 (also: ICASE Report 90-46 1990)
- [31] G.I. TAYLOR, *Stability of a viscous liquid contained between two rotating cylinders*. Phil. Trans. R. Soc. A 343 (1923) 223-289.
- [32] J. TEIXEIRA AND S. CHEINET, *A New Mixing Length Formulation for the Eddy-Diffusivity Closure*, Naval Research Laboratory Memorandum Report NRL/MR/7532-01-7244, NRL, Monterey, CA, May 2001, 25 pp.
- [33] J. TEIXEIRA AND S. CHEINET, *A Simple Mixing Length Formulation for the Eddy-Diffusivity Parameterization of Dry Convection*, Boundary-Layer Meteorology 110, 435–453 (2004). <https://doi.org/10.1023/B:BOUN.0000007230.96303.0d>
- [34] J. TEIXEIRA, J.P. FERREIRA, P.M. MIRANDA, T. HAACK, J. DOYLE, A.P. SIEBSEMA AND R. SALGADO, *A new mixing-length formulation for the parameterization of dry convection: implementation and evaluation in a mesoscale model*. Monthly weather review. 2004 Nov;132(11):2698-707.
- [35] J.C. VASSILICOS, *Dissipation in turbulent flows*, Ann. Rev. Fluid Mech. 47 (2015) 95-114.
- [36] X. WANG, *The time averaged energy dissipation rates for shear flows*, Physica D, 99 (1997) 555-563. 2004.
- [37] X. WANG, *Effect of tangential derivative in the boundary layer on time averaged energy dissipation rate*, Physica D: Nonlinear Phenomena 144 (2000), 142–153.
- [38] D.C. WILCOX, *Turbulence Modeling for CFD*, DCW Industries, La Canada, 2006.

## 7. APPENDIX: EXISTENCE OF LONG TIME LIMITS

In this appendix,  $C$  will denote any quantity uniformly bounded in time. We now prove the bounds given in Section 2 on

$$\begin{aligned} & \|v(T)\|^2, \int_{\Omega} k(T)dx, \int_{\Omega} \nu_T(\cdot, T)dx, \left\langle \frac{1}{L^3} \int_{\Omega} |\nabla^s v|^2 dx \right\rangle_T, \\ & \left\langle \frac{1}{L^3} \int_{\Omega} \frac{1}{l} k \sqrt{k} dx \right\rangle_T \quad \text{and} \quad \left\langle \frac{1}{L^3} \int_{\Omega} [2\nu + \nu_T(\cdot)] |\nabla^s v|^2 dx \right\rangle_T. \end{aligned}$$

**proof:** We begin with the energy equalities and inequalities for the two equations:

$$\begin{aligned} & \frac{1}{2} \frac{d}{dt} \|v\|^2 + \int_{\Omega} [2\nu + \nu_T(\cdot)] |\nabla^s v|^2 dx \leq \\ & \leq (v_t, \phi) + \int_{\Omega} [2\nu + \nu_T(\cdot)] \nabla^s v : \nabla^s \phi dx + (v \cdot \nabla v, \phi), \\ & \text{and} \quad \int_{\Omega} k_t dx + \int_{\Omega} \frac{1}{l} k \sqrt{k} dx = \int_{\Omega} \nu_T(\cdot) |\nabla^s v|^2 dx. \end{aligned}$$

Pick  $\theta, 0 < \theta < 1$ , and add the first equation +  $\theta \times$  second equation. Using  $\frac{d}{dt} \|\phi\|^2 = 0$  gives

$$\begin{aligned} & \frac{d}{dt} \left( \frac{1}{2} \|v\|^2 - (v, \phi) + \frac{1}{2} \|\phi\|^2 + \theta \int_{\Omega} k dx \right) + \\ (15) \quad & + \int_{\Omega} [2\nu + (1 - \theta)\nu_T(\cdot)] |\nabla^s v|^2 + \theta \frac{1}{l} k \sqrt{k} dx \leq \\ & \leq \int_{\Omega} [2\nu + \nu_T(\cdot)] \nabla^s v : \nabla^s \phi dx + (v \cdot \nabla v, \phi). \end{aligned}$$

We make the same choice of  $\phi$  only with  $\beta = \frac{1}{8} \mathcal{R}e^{-1}$  rather than  $\beta = \frac{1}{8} \mathcal{R}e_{eff}^{-1}$ . Consider now the three terms on the RHS. For the last, nonlinear term, we have proven the estimate

$$(v \cdot \nabla v, \phi) \leq C + \beta \mathcal{R}e \int_{\mathcal{S}_{\beta}} 2\nu |\nabla^s v|^2 dx \leq C + \frac{1}{8} \int_{\Omega} 2\nu |\nabla^s v|^2 dx,$$

and the second term is subsumed in the LHS of (15). The first term on the RHS is bounded by the Cauchy-Schwarz-Young inequality in a standard way as

$$\int_{\Omega} 2\nu \nabla^s v : \nabla^s \phi dx \leq C + \frac{1}{8} \int_{\Omega} 2\nu |\nabla^s v|^2 dx$$

with the second term on the RHS again subsumed as above. The remaining term on the RHS involves  $\nu_T$ . As a first step we again apply the Cauchy-Schwarz-Young inequality in a standard way and then use the direct calculation of  $|\nabla^s \phi|^2$  to give

$$\begin{aligned} \int_{\Omega} \nu_T(\cdot) \nabla^s v : \nabla^s \phi dx & \leq \frac{1 - \theta}{2} \int_{\Omega} \nu_T(\cdot) |\nabla^s v|^2 dx + \frac{1}{2(1 - \theta)} \int_{\Omega} \nu_T(\cdot) |\nabla^s \phi|^2 dx \\ & \leq \frac{1 - \theta}{2} \int_{\Omega} \nu_T(\cdot) |\nabla^s v|^2 dx + \frac{\mu}{2(1 - \theta)} \left( \frac{U}{\beta L} \right)^2 \int_{\mathcal{S}_{\beta}} l \sqrt{k} dx. \end{aligned}$$

Collecting these terms in (15) gives

$$\begin{aligned} \frac{d}{dt} \left( \frac{1}{2} \|v - \phi\|^2 + \theta \int_{\Omega} k dx \right) + \int_{\Omega} \left[ \frac{3}{2} \nu + \frac{1-\theta}{2} \nu_T(\cdot) \right] |\nabla^s v|^2 + \theta \frac{1}{l} k \sqrt{k} dx &\leq \\ &\leq C + \frac{\mu}{2(1-\theta)} \left( \frac{U}{\beta L} \right)^2 \int_{S_{\beta}} l \sqrt{k} dx. \end{aligned}$$

For the last term we apply Hölder's inequality with exponents 3 and 3/2 as follows

$$\begin{aligned} \int_{S_{\beta}} l \sqrt{k} dx &= \int_{S_{\beta}} l^{4/3} \cdot l^{-1/3} \sqrt{k} dx \leq \left( \int_{S_{\beta}} l^{-1} k^{3/2} dx \right)^{\frac{1}{3}} \left( \int_{S_{\beta}} (l^{4/3})^{3/2} dx \right)^{\frac{2}{3}} \\ \frac{1}{2(1-\theta)} \left( \frac{U}{\beta L} \right)^2 \int_{S_{\beta}} \mu l \sqrt{k} dx &\leq \frac{1}{3} \int_{\Omega} \frac{1}{l} k \sqrt{k} dx + \frac{2}{3} \left[ \frac{1}{2(1-\theta)} \left( \frac{U}{\beta L} \right)^2 \right]^{3/2} \int_{S_{\beta}} l^2 dx. \end{aligned}$$

We thus have

$$(16) \quad \begin{aligned} &\frac{d}{dt} \left( \frac{1}{2} \|v - \phi\|^2 + \theta \int_{\Omega} k dx \right) + \\ &+ \int_{\Omega} \left[ \frac{3}{2} \nu + \frac{1-\theta}{2} \nu_T(\cdot) \right] |\nabla^s v|^2 + \theta \frac{1}{l} k \sqrt{k} dx \leq C + C^* \int_{S_{\beta}} l^2 dx, \end{aligned}$$

where

$$C^* = \frac{2}{3} \left[ \frac{1}{2(1-\theta)} \right]^{3/2} \left( \frac{U}{\beta L} \right)^3.$$

The result now follows by standard differential inequalities provided there is an  $\alpha > 0$  with

$$\int_{\Omega} \frac{1}{l} k \sqrt{k} dx \geq \alpha \int_{\Omega} k dx \quad \text{and} \quad \int_{S_{\beta}} l^2 dx \leq C < \infty.$$

These two depend on the choice of  $l = \min \left\{ \sqrt{2} k^{1/2} \tau, 0.41 d \sqrt{\frac{d}{L}} \right\}$ . By selecting the last argument in the minimum, the condition  $\int l^2 dx \leq C < \infty$  holds. By selecting the first term in the minimum (and noting that then  $\frac{1}{l} k \sqrt{k} = \frac{1}{\sqrt{2} \tau} k$ ) the condition  $\int \frac{1}{l} k \sqrt{k} dx \geq \alpha \int k dx$  holds. Thus the uniform bounds follows.

<sup>1</sup>DEPARTMENT OF MATHEMATICS, UNIVERSITY OF PITTSBURGH, PITTSBURGH PA 15260, USA,

<sup>2</sup>DEPARTMENT OF MATHEMATICS, UNIVERSITY OF PITTSBURGH, PITTSBURGH PA 15260, USA,

<sup>3</sup>DEPARTMENT OF MATHEMATICS, UNIVERSITY OF PITTSBURGH, PITTSBURGH PA 15260, USA

*Email address:* kkh16@pitt.edu<sup>1</sup>, wjl@pitt.edu<sup>2</sup>, mhs64@pitt.edu<sup>3</sup>